Aryl Sulfoxide Radical Cations. Generation, Spectral Properties, and Theoretical Calculations

Enrico Baciocchi,[†] Tiziana Del Giacco,*[,‡] Maria Francesca Gerini,[†] and Osvaldo Lanzalunga*[,†]

Dipartimento di Chimica, Università degli Studi di Roma "La Sapienza" and Istituto CNR di Metodologie Chimiche (IMC-CNR), Sezione Meccanismi di Reazione, P.le A. Moro, 5 I-00185 Rome, Italy, and Dipartimento di Chimica and Centro di Eccellenza Materiali Innovativi Nanostrutturati (CEMIN), Università di Perugia, Via Elce di Sotto 8, 06123 Perugia, Italy

Received: April 20, 2006; In Final Form: June 12, 2006

Aromatic sulfoxide radical cations have been generated by pulse radiolysis and laser flash photolysis techniques. In water (pulse radiolysis) the radical cations showed an intense absorption band in the UV region (ca. 300 nm) and a broad less intense band in the visible region (from 500 to 1000 nm) whose position depends on the nature of the ring substituent. At very low pulse energy, the radical cations decayed by first-order kinetics, the decay rate increasing as the pH increases. It is suggested that the decay involves a nucleophilic attack of H_2O or OH^- (in basic solutions) to the positively charged sulfur atom to give the radical $ArSO(OH)CH_3^{\bullet}$. By sensitized [*N*-methylquinolinium tetrafluoborate (NMQ^+)] laser flash photolysis (LFP) the aromatic sulfoxide radical cations were generated in acetonitrile. In these experiments, however, only the band of the radical cation in the visible region could be observed, the UV band being covered by the UV absorption of NMQ^+. The λ_{max} values of the bands in the visible region resulted almost identical to those observed in water for the same radical cations. In the LFP experiments the sulfoxide radical cations decayed by second-order kinetics at a diffusion-controlled rate, and the decay is attributed to the back electron transfer between the radical cation and $NMQ^{\bullet}$. DFT calculations were also carried out for a number of 4-X ring substituted (X = H, Me, Br, OMe, CN) aromatic sulfoxide radical cations (and their neutral parents). In all radical cations, the conformation with the S−O bond almost coplanar with the aromatic ring is the only one corresponding to the energy minimum. The maximum of energy corresponds to the conformation where the S−O bond is perpendicular to the aromatic ring. The rotational energy barriers are not very high, ranging from 3.9 to 6.9 kcal/mol. In all radical cations, the major fraction of charge and spin density is localized on the SOMe group. However, a substantial delocalization of charge and spin on the ring (almost 50% for the 4-methoxy derivative and around 30% for the other radical cations) is also observed. This suggests some conjugative interaction between the MeSO group and the aromatic system that may become very significant when a strong electron donating substituent like the MeO group is present. The ionization energies (IE) of the 4-X ring substituted neutral aromatic sulfoxides were also calculated, which were found to satisfactorily correlate with the experimental E_p potentials measured by cyclic voltammetry.

Introduction

Sulfoxide is a functional group of great interest for its importance in organic synthesis[1] as well as for the biological activity and its involvement in the general metabolism of many biologically important sulfides.[2] Thus, the reactivity of sulfoxides in polar, radical, and photochemical processes has been the object of much investigation.[3] In contrast, the behavior of sulfoxides in electron transfer oxidation reactions has been little studied, probably due to the relatively high oxidation potential of these species.[4] Consequently, little is known about sulfoxide radical cations, the few studies presently available exclusively concerning dialkyl sulfoxide radical cations.[5] Very surprisingly, almost nothing[6−8] is known about aromatic sulfoxide radical cations, while these species, having a redox potential lower than that of the dialkyl counterparts,[4] should have more chances to be involved in oxidative chemical and biochemical transformations. In this respect, it is useful to mention that an electron-transfer process has been suggested in the oxidation of aromatic sulfoxides by cytochrome P-450.[9] Moreover, according to recent results[7,8] also the reaction of aromatic sulfoxides with iron(III)− and ruthenium(III)−polypiridyl complexes seems to involve an electron-transfer mechanism.

In view of our continuous involvement in radical cations chemistry,[10] we have considered it of interest to devote our attention to aromatic sulfoxide radical cations, and in this paper we now report on a pulse radiolysis and flash photolysis study concerning generation and spectral properties of the radical cations of a number of aromatic sulfoxides (Chart 1). DFT calculations providing geometrical properties, rotational barriers around the ArS(O)−C bond, charges, and spin densities are also reported. For comparison purpose calculations have been carried out also on the parent sulfoxides. As far as we know this is the first study describing spectral properties and main structural features of aromatic sulfoxide radical cations.

* Corresponding author e-mail: osvaldo.lanzalunga@uniroma1.it and dgiacco@unipg.it.

[†] Università degli Studi di Roma "La Sapienza" and Istituto CNR di Metodologie Chimiche (IMC-CNR).

[‡] Università di Perugia.

10.1021/jp0624350 CCC: $33.50
Published on Web 07/15/2006

CHART 1

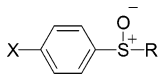

1 X = H, R = CH_3
2 X = OCH_3, R = CH_3
3 X = CH_3, R = CH_3
4 X = Br, R = CH_3
5 X = CN, R = CH_3
6 X = H, R = $C(CH_3)_3$

Generation and Absorption Spectra of Aromatic Sulfoxide Radical Cations

(a) Pulse Radiolysis Experiments in H_2O. The radical cations $\mathbf{1}^{\bullet+}-\mathbf{5}^{\bullet+}$ were generated from the parent sulfoxides as described by Kishore and Asmus for the dialkyl sulfoxide radical cations.[11] Namely, $\mathbf{1}^{\bullet+}-\mathbf{5}^{\bullet+}$ were produced by pulse radiolysis, in argon-saturated aqueous solution containing 2-methyl-2-propanol (0.5 M) at pH 4.0, by reaction of **1**−**5** with the strongly oxidizing sulfate radical anion ($SO_4^{\bullet-}$) ($E°$ ca. 2.5 V vs NHE)[12] (eqs 1−4).

$$H_2O \rightsquigarrow H^+, {}^\bullet OH, e^-_{aq} \quad (1)$$

$$^\bullet OH + CH_3C(CH_3)_2OH \rightarrow H_2O + {}^\bullet CH_2C(CH_3)_2OH \quad (2)$$

$$e^-_{aq} + S_2O_8^{2-} \rightarrow SO_4^{2-} + SO_4^{\bullet-} \quad (3)$$

$$SO_4^{\bullet-} + ArSOCH_3 \rightarrow SO_4^{2-} + ArSOCH_3^{\bullet+} \quad (4)$$

The hydroxyl radical ($^\bullet$OH) is scavenged by 2-methyl-2-propanol (eq 2) with $k = 6 \times 10^8$ M^{-1} s^{-1},[13] while the hydrated electron (e_{aq}^-) reacts with the peroxydisulfate anion leading to the formation of $SO_4^{\bullet-}$ (eq 3), with $k = 1.2 \times 10^{10}$ M^{-1} s^{-1}.[13] The absorption spectrum observed for the reaction of **3** recorded 10 μs after the electron pulse is displayed in Figure 1. The absorption spectra of radical cations $\mathbf{1}^{\bullet+}$, $\mathbf{2}^{\bullet+}$, $\mathbf{4}^{\bullet+}$, and $\mathbf{5}^{\bullet+}$ are reported in Figures S1−S4 in the Supporting Information.[14]

With all sulfoxides, the absorption spectra showed an intense absorption band in the UV region and a broad less intense band in the visible region (500−1000 nm) whose position appears to depend on the nature of the ring substituent. The two bands decay with the same rate, so they belong to the same species, the sulfoxide radical cation. As expected for a radical cation, the two bands are unaffected by the presence of oxygen.

It is interesting to note that only the UV band was observed by Kishore and Asmus for dialkyl sulfoxide radical cations,[11] which suggests that the additional visible absorption bands observed for $\mathbf{1}^{\bullet+}-\mathbf{5}^{\bullet+}$ should be associated with an electronic transition involving the aromatic moiety.[15]

The λ_{max} values for the absorptions of radical cations $\mathbf{1}^{\bullet+}-\mathbf{5}^{\bullet+}$ are collected in Table 1. As already noted, the position of the absorption band in the visible region is influenced by the nature of the ring substituent. In particular, with respect to $\mathbf{1}^{\bullet+}$, λ_{max} of this band increases in the presence of either electron withdrawing (EW) ($\mathbf{4}^{\bullet+}$, $\mathbf{5}^{\bullet+}$) or electron donating (ED) ($\mathbf{2}^{\bullet+}$, $\mathbf{3}^{\bullet+}$) para ring substituents, the higher effects being observed with the strong ED 4-MeO group. Kishore and Asmus have suggested that sulfoxide radical cations in water are probably associated with a molecule of water.[11] This possibility seems unlikely for aromatic sulfoxide radical cations since, as we will see later, the λ_{max} value of the visible band remains practically unchanged when water is replaced by MeCN, as the solvent. If a radical cation−water complex is formed also with aromatic sulfoxide radical cations it should be a very loose complex.

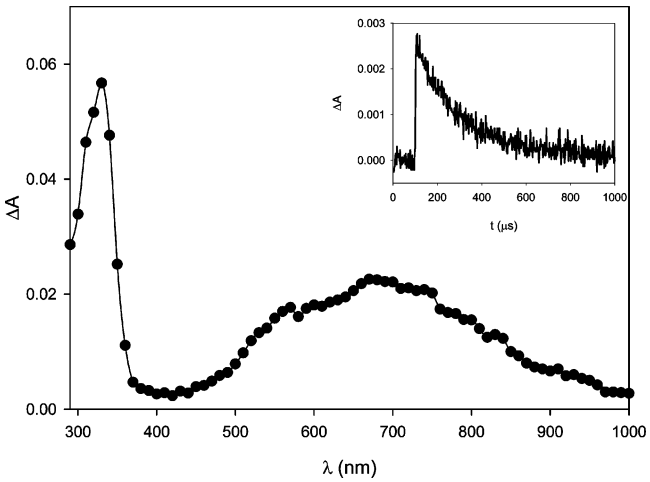

Figure 1. UV−vis absorption spectrum of radical cation $\mathbf{3}^{\bullet+}$ observed on reaction of $SO_4^{\bullet-}$ with **3** (0.5 mM) at $T = 25$ °C, recorded after pulse radiolysis of an Ar-saturated aqueous solution at pH = 4.0, containing 0.5 M 2-methyl-2-propanol at 10 μs after the 2 μs, 10-MeV electron pulse. Inset: decay of the absorption at 670 nm recorded after a 0.2 μs, 10-MeV electron pulse.

TABLE 1: Optical Absorption Peaks, Rate Constants for the Decay of the Radical Cations of Aromatic Sulfoxides $\mathbf{1}^{\bullet+}-\mathbf{5}^{\bullet+}$ Generated by Pulse Radiolysis of Aqueous Solution at pH 4.0 under Argon Measured at $T = 25$ °C, and Experimental Peak Reduction Potential of $\mathbf{1}^{\bullet+}-\mathbf{5}^{\bullet+}$

radical cation	λ_{max}/(nm)[a]	k (s^{-1})[b]	E_p (V vs SCE)[c]
$\mathbf{1}^{\bullet+}$	320,550	4.0×10^3	2.01
$\mathbf{2}^{\bullet+}$	300,900	2.8×10^3	1.90
$\mathbf{3}^{\bullet+}$	330,670	3.8×10^3	1.95
$\mathbf{4}^{\bullet+}$	340,660	1.4×10^4	2.06
$\mathbf{5}^{\bullet+}$	330,560	6.8×10^4	2.16

[a] Doses 20 Gy/pulse. [b] Doses 2 Gy/pulse. [c] Determined by cyclic voltammetry in MeCN, Bu_4NBF_4 (0.1 M) as the supporting electrolyte. [sulfoxide] = 2.0 mM. Voltage sweep rate 500 mV/s^{-1}.

The time-evolution of the absorption spectra showed that for all radical cations, the decay of the two bands is not accompanied by the buildup of any transient absorbing significantly in the UV−vis region of the spectrum. The decay rate of $\mathbf{1}^{\bullet+}-\mathbf{5}^{\bullet+}$, measured spectrophotometrically by following the change in optical density at the wavelengths corresponding to the absorption maxima, was found to be dose dependent. At higher doses, the radical cations were found to decay by a mixed first-second-order reaction, whereas at the lowest dose (ca. 2 Gy/pulse), the decays fitted first-order kinetics (see insets of Figures 1 and S1−S4 in the Supporting Information). It was also found that the decay rate is pH dependent, increasing as pH increases. Namely, the decay rate of $\mathbf{1}^{\bullet+}$ increases from 7.1 $\times 10^3$ s^{-1} at pH 4.5 to 1.2 $\times 10^5$ s^{-1} at pH 9.1 (see Figure S5 in the Supporting Information). However, we found that the yield in radical cation does not decrease by increasing pH as instead it was observed for dialkyl sulfoxide radical cations (Figure S5). We will comment on this point later on.

The first-order rate constants (k_1) for the decay of $\mathbf{1}^{\bullet+}-\mathbf{5}^{\bullet+}$ determined at low doses at pH 4 are reported in Table 1. In the same table are also displayed the peak reduction potentials of the radical cations which have been measured by cyclic voltammetry (see the Supporting Information). By looking at these data, it can be observed that the rate of decay increases as the reduction potential of the radical cation becomes higher, that is as the radical cation becomes less stable.

Concerning the nature of the decay, the increase in the decay rate by increasing pH clearly suggests a reaction of the radical

cation with H_2O in acidic solution and a faster reaction with hydroxide ion in basic solution. Since we found similar decay rates for $C_6H_5SOCH_3^{\bullet+}$ and $C_6H_5SOCD_3^{\bullet+}$ in the 4.0−9.1 pH range (Figure S5 in the Supporting Information), it can be excluded that the decay involves deprotonation at the SOMe methyl group. Thus it is very likely that the decays of **1**$^{\bullet+}$−**5**$^{\bullet+}$ involve the nucleophilic attack of H_2O (at pH 4) or OH^- (at pH 9) to the positively charged sulfur atom to give the radical $ArSO(OH)CH_3^{\bullet}$ (eq 5), as suggested by Kishore and Asmus for dialkyl sulfoxide radical cations.[11]

$$ArSOCH_3^{\bullet+} + OH^-(H_2O) \longrightarrow ArS(O^{\bullet})(OH)CH_3 \ (+H^+) \quad (5)$$

An interesting observation is that the radical cation yield (measured for **1**$^{\bullet+}$) resulted pH independent in the 4.0−9.1 pH range, a result contrasting with what was observed for dialkyl sulfoxide radical cations where the radical cation yield significantly decreased by increasing the pH from 5.0 to 8.0. A possible explanation is that in aromatic sulfoxide radical cations a substantial part of the positive charge is delocalized in the aromatic ring (vide infra). Thus, the nucleophilic attack of H_2O/OH^- is probably much slower than with dialkyl sulfoxide radical cations and can be followed on the μs time scale.

(b) Laser Flash Photolysis in MeCN. In the photochemical studies radical cations were generated by sensitized laser flash photolysis ($\lambda_{exc} = 355$ nm) in MeCN with *N*-methylquinolinium tetrafluoborate (NMQ^+) as the sensitizer. NMQ^+ is a very efficient sensitizer whose excited state ($^1NMQ^{+*}$) is characterized by a very high reduction potential (2.7 V vs SCE),[16] much higher than the oxidation potential of the aromatic sulfoxides **1**−**5** (around 2.0 V vs SCE, see Table 1).[4] Toluene (1 M) was used as cosensitizer to reduce the efficiency of the back-electron-transfer process (eqs 6 and 7) and, consequently, to increase the concentration of the transient formed within the laser pulse.[17]

$$^1NMQ^{*+} + C_6H_5CH_3 \rightarrow NMQ^{\bullet} + C_6H_5CH_3^{\bullet+} \quad (6)$$

$$C_6H_5CH_3^{\bullet+} + ArSOCH_3 \rightarrow C_6H_5CH_3 + ArSOCH_3^{\bullet+} \quad (7)$$

Under these conditions, however, because of the strong absorption of the sensitizer, our observation was necessarily limited to the $\lambda > 360$ nm region of the spectrum. Thus, the laser photolysis of sulfoxides **1**−**5** solutions produced spectra where only the band of the radical cation in the visible region of the spectrum could be observed. In deaerated MeCN, this band overlapped to various extents with the absorptions at 400 and 540 nm due to the reduced *N*-methylquinolinium ($NMQ^{\bullet}$)[19] (see Figures S6−S10 in the Supporting Information). Thus, the laser photolysis experiments were carried out in the presence of oxygen that, by quenching of $NMQ^{\bullet}$,[16] permitted in all cases the clear observation of the visible absorption of the aromatic sulfoxide radical cations. As an example, the spectrum obtained by the laser photolysis of **3** in O_2-saturated CH_3CN is reported in Figure 2. The absorption spectra of the radical cations **1**$^{\bullet+}$, **2**$^{\bullet+}$, **4**$^{\bullet+}$, and **5**$^{\bullet+}$ are similar to that of **3**$^{\bullet+}$ and are reported in Figures S11−S14 in the Supporting Information. For each radical cation, the λ_{max} value (Table 2) resulted almost identical to that found for the visible absorption band in water in the pulse radiolysis experiments.

To further support the assignment of the observed absorption to the sulfoxide radical cation, the laser photolysis of **3** (2.1×10^{-2} M) was carried out in the presence of 1,4-dimethoxybenzene (DMB) (2.9×10^{-4} M). It was found that the 680 nm absorption, observed 80 ns after the laser pulse, is replaced, after 3 μs, by the spectrum of DMB radical cation ($\lambda_{max} = 430$ and 460 nm)[20] as clearly shown in Figure 3. Thus the initially generated **3**$^{\bullet+}$ ($E_p = 1.95$ V vs SCE) is successively reduced by DMB ($E = 1.3$ V vs SCE).[21]

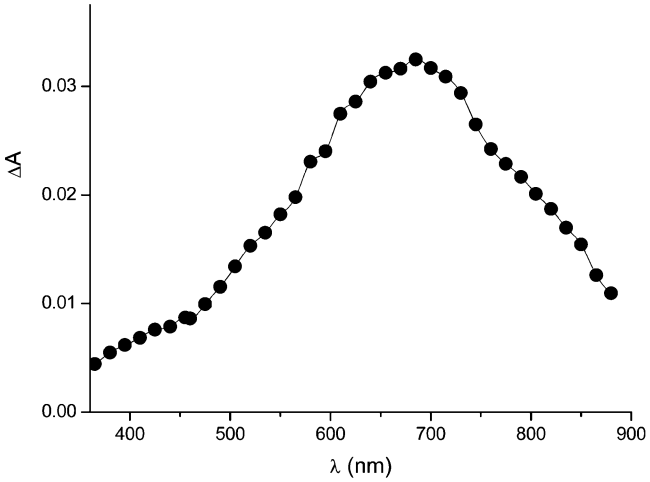

Figure 2. Absorption spectra of the NMQ^+ (3.9×10^{-3} M)/toluene (1 M)/4-$CH_3C_6H_4SOCH_3$ (1.5×10^{-2} M) system in O_2-saturated CH_3CN recorded 80 ns after the laser pulse. $\lambda_{exc} = 355$ nm.

TABLE 2: Spectral Data and Decay Rate Constants for the Radical Cations of Aromatic Sulfoxides 1$^{\bullet+}$−5$^{\bullet+}$ Generated by Laser Flash Photolysis of the NMQ^+/1−5 System in CH_3CN

radical cation	λ_{max}/(nm)[a]	ϵ_{max}/($M^{-1}cm^{-1}$)[b]	$2k_2/\epsilon$ ($s^{-1}cm$)[b]	k_2 ($M^{-1}s^{-1}$)
1$^{\bullet+}$	550	nd[c]	3.6×10^7	
2$^{\bullet+}$	900	6400	2.1×10^7	6.7×10^{10}
3$^{\bullet+}$	670	3050	3.8×10^7	5.8×10^{10}
4$^{\bullet+}$	660	1930	3.1×10^7	3.0×10^{10}
5$^{\bullet+}$	550	nd[c]	1.8×10^7	

[a] In O_2-saturated CH_3CN, in the presence of toluene (1 M). [b] In N_2-saturated CH_3CN. [c] Not determined due to the superimposition of the visible absorption band of the radical cation with that of $NMQ^{\bullet}$ ($\lambda_{max} = 540$ nm).

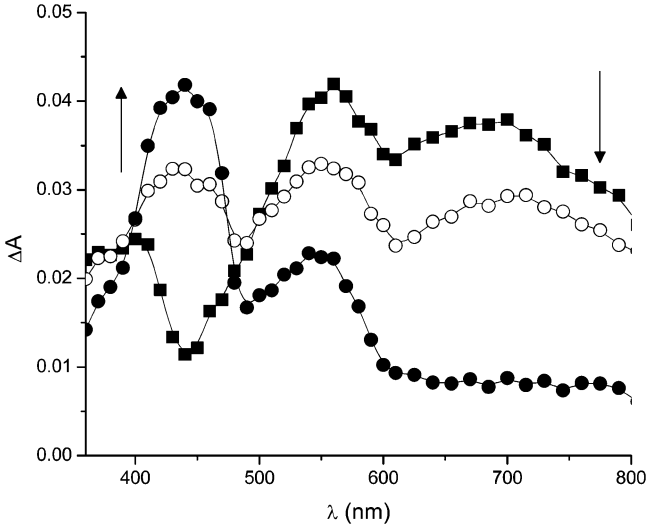

Figure 3. Absorption spectra of the NMQ^+ (3.9×10^{-3} M)/toluene (1 M)/4-$CH_3C_6H_4SOCH_3$ (2.1×10^{-2} M) system in N_2-saturated CH_3CN in the presence of 1,4-dimethoxybenzene (2.9×10^{-4} M) recorded 40 ns (filled squares), 180 ns (empty circles), and 3.1 μs (filled circles) after the laser pulse. $\lambda_{exc} = 355$ nm.

For the radical cations $\mathbf{2}^{\bullet+}-\mathbf{4}^{\bullet+}$ the absorption bands resulted well separated from the absorption band of $NMQ^{\bullet}$ ($\lambda_{max} = 540$ nm) and could be observed also in deaerated MeCN. Under these conditions, considering that the radical cation and $NMQ^{\bullet}$ are formed in equimolar amounts and that the extinction coefficient at 540 nm of $NMQ^{\bullet}$ is known ($\epsilon = 3600\ M^{-1}\ cm^{-1}$),[22] it was possible to determine the molar extinction coefficients for the absorptions of $\mathbf{2}^{\bullet+}-\mathbf{4}^{\bullet+}$. These values are collected in Table 2.

The decay rates of radical cations $\mathbf{1}^{\bullet+}-\mathbf{5}^{\bullet+}$ were determined under nitrogen and in the absence of toluene, by following the change in optical density at the wavelengths corresponding to the absorption maxima listed in Table 2. No buildup of any transient was observed, and the decay rates followed second-order kinetics (see Figures S15−S19 in the Supporting Information). For $\mathbf{2}^{\bullet+}-\mathbf{4}^{\bullet+}$ similar decay rates were determined for the radical cation and $NMQ^{\bullet}$. The decay rate constants (k_2), divided by the extinction coefficient (ϵ), for all the radical cations, are reported in Table 2; for $\mathbf{2}^{\bullet+}-\mathbf{4}^{\bullet+}$ the k_2 values are also reported which suggest a diffusion-controlled process. These results can be reasonably interpreted on the basis of a decay process dominated by a back electron transfer between the radical cation and $NMQ^{\bullet}$. In agreement with this conclusion, only unreacted sulfoxide was recovered in the NMQ^{+} sensitized steady-state photolysis of sulfoxide **3**.

DFT Calculations

DFT calculations, performed with the Gaussian 98 program[24] using the three-parameter hybrid functional B3LYP[25] with the 6-311G* basis set,[26] were carried out in order to obtain data on the conformational equilibria, energy barriers for the internal rotation, geometry, charge, and spin distributions on the investigated alkyl aryl sulfoxide both in the neutral and in the radical cation forms. The DFT method was chosen because it provides results for open-shell species that are often in better agreement with the available experimental data than HF or MP2 calculations.[27] DFT calculations are more attractive also with respect to the very costly coupled cluster and quadratic configuration interaction methods. The potential energy for the internal rotation was calculated as a function of the dihedral angles $C_{Ar2}-C_{Ar1}-S-O$ (ϕ_1) and $C_{Ar2}-C_{Ar1}-S-C_{Alk}$ (ϕ_2) by varying it by steps of 30° (or for some molecules at shorter intervals to better define the shape of the potential barrier) and allowing the other parameters to be optimized. The minima and maxima on the torsional potential were optimized. Harmonic vibrational frequencies were calculated at the B3LYP/6-311G* level to confirm that optimized structures correspond to local minima and to determine zero-point energy (ZPE) corrections. The barriers for internal rotations were calculated as the differences between the total energy of each conformation and that of the most stable conformer. Atomic charges and unpaired electron spin densities were calculated using the Mulliken population analysis.

(a) Neutral Sulfoxides. The B3LYP/6-311G* calculations on neutral C_6H_5SOMe located the energy minimum on the potential function at the conformation with the dihedral angle $C_{Ar2}-C_{Ar1}-S-O$ (ϕ_1) 7° below the aromatic ring plane and the dihedral angle $C_{Ar2}-C_{Ar1}-S-CH_3$ (ϕ_2) 80° above the plane, Figure 4, conformation **1a**. The maximum of energy was obtained for the conformation with the $S-CH_3$ bond coplanar with the aromatic ring and $\phi_1 = 120°$ (Figure 4, conformation **1b**). In all conformers the sulfur atom always retains a pyramidal geometry with a dihedral angle of 30°.

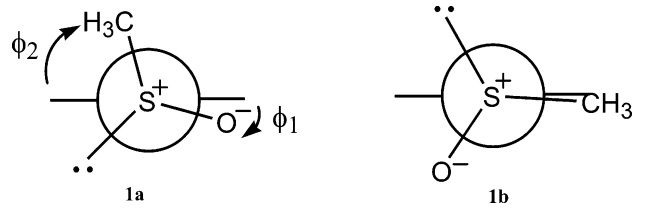

Figure 4. C_6H_5SOMe conformers at the minimum (a) and at the maximum of energy (b) in the rotation around the $C_{Ar}-S$ bond.

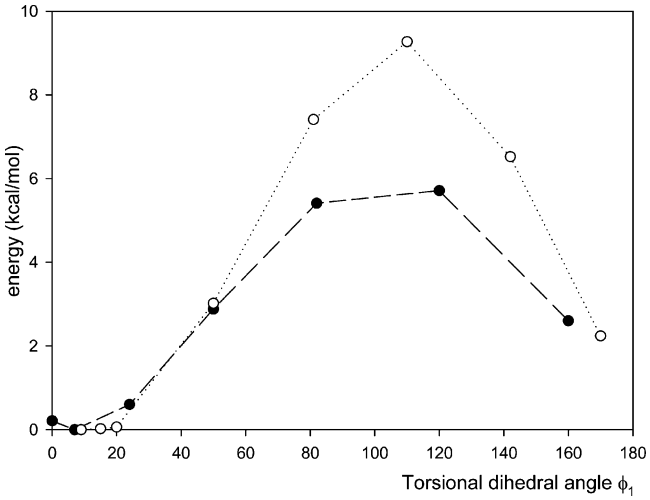

Figure 5. Energy profiles for the internal rotation about the $C_{Ar}-S$ bond in C_6H_5SOMe (**1**) (filled circles) and C_6H_5SOtBu (**6**) (empty circles).

The energy profile for the internal rotation about the $C_{Ar}-S$ bond in neutral C_6H_5SOMe (**1**) is reported in Figure 5 (filled circles).

The calculated energy barrier for rotation around the $C_{Ar1}-S$ bond, 6.0 kcal/mol, is in very good agreement with experimental observations indicating that such a barrier should not exceed 6 kcal/mol.[28] In this respect, our results compare well with those of previous calculations. Thus, a rotational barrier of 5.1 kcal/mol has been recently obtained by MP2/6-31G* calculations,[29] whereas a slightly higher value (8.3 kcal/mol) has been reported by Benassi et al.[30] Full optimization of the geometric parameters by MP2/6-31G* calculations[29] showed that the energy minimum conformation of C_6H_5SOMe is reached at $\phi_2 = 75°$ and the energy maximum at $\phi_2 = 180°$. Thus the preferred conformation corresponds to an SO bond nearly eclipsed with the phenyl ring as also suggested by Butenko et al.[31]

The conformational features of the sulfoxide appear to be slightly sensitive to the bulkiness of the alkyl group. Thus, in C_6H_5SOtBu (**6**) conformation at the minimum of energy has the dihedral angle $C_{Ar2}-C_{Ar1}-S-O$ (ϕ_1) 9° below the aromatic ring plane and the dihedral angle $C_{Ar2}-C_{Ar1}-S$-*t*Bu (ϕ_2) 100° above the plane, and the sulfur atom always retains a pyramidal geometry with a dihedral angle of 30°. The energy profile for rotation around the $C_{Ar1}-S$ bond of C_6H_5SOtBu is shown in Figure 4 (empty circles). The maximum is found for the conformation with the *tert*-butyl group in the planar position and $\phi_1 = 110°$. The rotational energy barrier, however, is higher than with C_6H_5SOMe, becoming 9.3 kcal/mol.

The shape of these energy profiles as well as the rotational energy barriers suggest that the conformational equilibrium should be mainly controlled by the interaction of the alkyl group with the ortho hydrogen atoms of the aromatic ring in the conformer where the S-alkyl bond is parallel to the ring plane (e.g. **1b** in Figure 4).

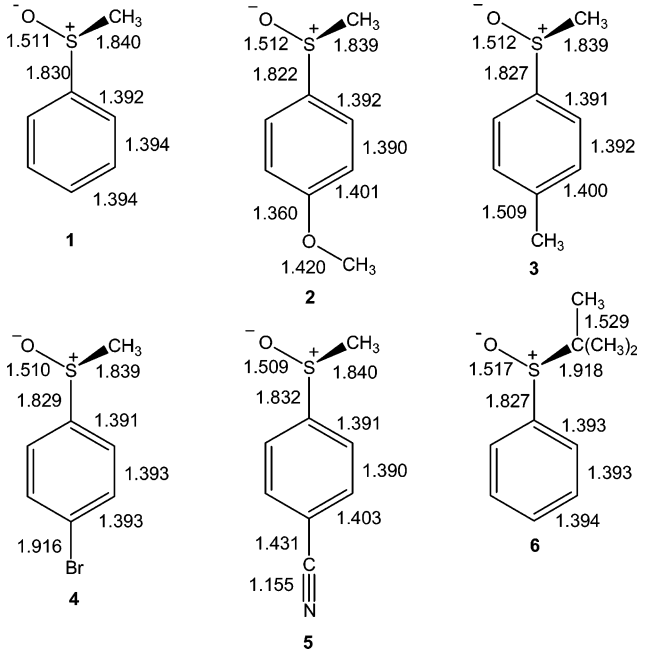

Figure 6. Bond lengths for the most stable ArSOR (**1**−**6**) conformers.

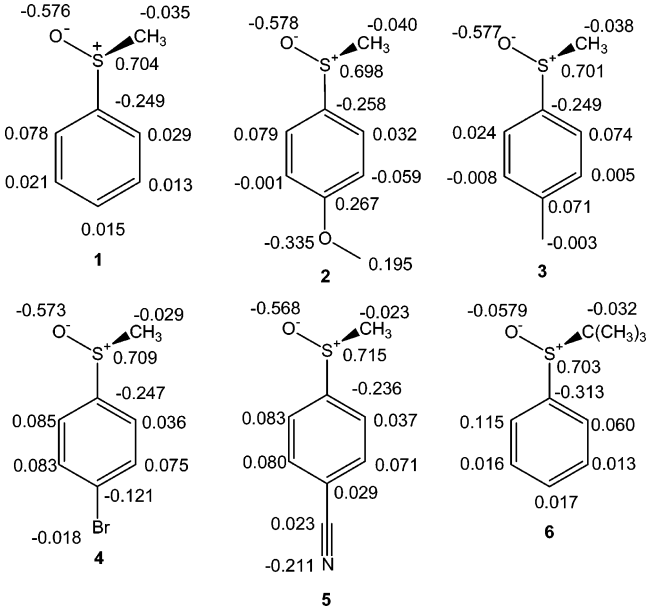

Figure 7. Mulliken charges for the most stable ArSOR (**1**−**6**) conformers (hydrogen atoms are summed into the attached carbon atoms).

The calculated bond distances in C_6H_5SOMe[32] and C_6H_5-SO*t*Bu are reported in Figure 6 together with the geometries of a number of para-substituted phenyl methyl sulfoxides (compounds **2**−**5** in Chart 1) in the minimum energy conformation.

It can be noted that the para substituent does not exert a significant effect upon the geometry of ArSOMe. Thus, both the C_{Ar1}−S and SO bond lengths remain practically unchanged in the presence of either electron withdrawing or donating substituents. This would suggest that there is no significant conjugative interaction between the ring and the SOMe group, a conclusion that appears confirmed by the fact that the SO bond length in dimethyl sulfoxide (1.509 Å)[33] is almost identical to that in C_6H_5SOMe (1.511 Å).[34] A contrary indication, however, seems to come from the observation that the charge distribution is affected by the nature of the para substituent (Figure 7). In particular, the positive charge density present in the SOMe group regularly increases as we move from electron donating to electron withdrawing substituents (MeO < Me < H < Br < CN). As a matter of fact, the positive charge density in the SOMe group is 0.093 in the unsubstituted sulfoxide, decreases to 0.080 in 4-$MeOC_6H_4SOMe$, but increases to 0.124 in 4-CNC_6H_4-SOMe. Thus, it would seem that SOMe group may to some extent behave as an electron donating group by a resonance effect involving the sulfur lone pair (Figure 8, structure **B**).

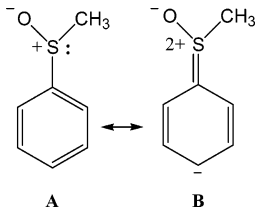

Figure 8.

Interestingly, a resonance effect of this type has been recently suggested by Rosini et al.[36] at least for aryl methyl sulfoxides with electron withdrawing substituents on the basis of UV and CD spectra. It can be added that, in line with the above reasoning, the MeSO group is an ortho−para orienting group in electrophilic aromatic substitutions.[37]

(b) Sulfoxide Radical Cations. *Conformational Studies and Bond Distances.* For $C_6H_5SOMe^{\bullet+}$ the energy minimum conformation (therefrom indicated as the stable conformation) corresponds to the conformer with $\phi_1 = 3°$ below the aromatic ring plane and $\phi_2 = 70°$ above the plane (**1**$^{\bullet+}$**a** in Figure 9), while the conformer with $\phi_1 = 90°$ and $\phi_2 = 150°$ is at a maximum in energy (**1**$^{\bullet+}$**b** in Figure 9). A very similar situation is observed with the para-substituted derivatives. In the radical cations too the sulfur atom always exhibits a pyramidal geometry with a dihedral angle of 30° in all the conformers.

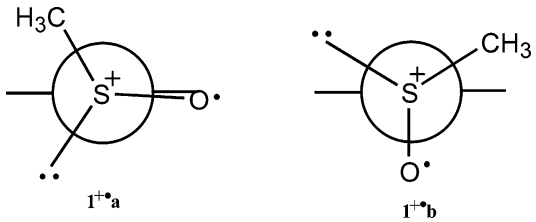

Figure 9. $C_6H_5SOMe^{\bullet+}$ conformers at the minimum (a) and at the maximum of energy (b) in the rotation around the C_{Ar}−S bond.

The energy profiles for the rotation around the C_{Ar1}−S bond are shown in Figure 10 for $C_6H_5SOMe^{\bullet+}$ (**1**$^{\bullet+}$), 4-$MeOC_6H_4$-$SOMe^{\bullet+}$ (**2**$^{\bullet+}$), 4-$MeC_6H_4SOMe^{\bullet+}$ (**3**$^{\bullet+}$), and 4-$CNC_6H_4SOMe^{\bullet+}$ (**5**$^{\bullet+}$). The rotational energy barrier is 3.9 kcal/mol for **5**$^{\bullet+}$, 4.0 kcal/mol for **1**$^{\bullet+}$, 5.1 kcal/mol for **3**$^{\bullet+}$, and 6.9 kcal/mol for **2**$^{\bullet+}$, slightly increasing as we move from electron withdrawing to electron donating substituents. The origin of this barrier is probably not steric, since steric interactions between the methyl group and ortho hydrogens should not be very different in conformations **1**$^{\bullet+}$**a** and **1**$^{\bullet+}$**b** (Figure 9). Electronic effects may be into play (vide infra).

The geometries of the stable conformations of the sulfoxide radical cations are reported in Figure 11. In all cases, these geometries do not significantly change on passing to the conformation at the maximum of energy, apart from a little increase (about 0.02 Å) in the S−O bond length (see Figure S20 in the Supporting Information for the two conformations **1**$^{\bullet+}$**a** and **1**$^{\bullet+}$**b**).

For what concerns the charge and spin density values reported in Figure 12 (Mulliken charges and spin populations), calculations indicate that in **1**$^{\bullet+}$ charge and spin are mainly (ca. 70%)

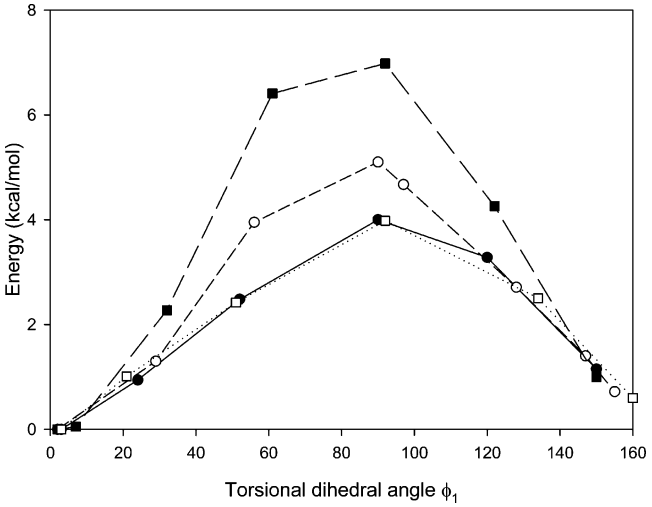

Figure 10. Energy profiles for the internal rotation about the $C_{Ar}-S$ bond in $C_6H_5SOMe^{\bullet+}$ (**1**$^{\bullet+}$) (filled circles), 4-$MeOC_6H_4SOMe^{\bullet+}$ (**2**$^{\bullet+}$) (filled squares), 4-$MeC_6H_4SOMe^{\bullet+}$ (**3**$^{\bullet+}$) (empty circles), and 4-CNC_6H_4-$SOMe^{\bullet+}$ (**5**$^{\bullet+}$) (empty squares).

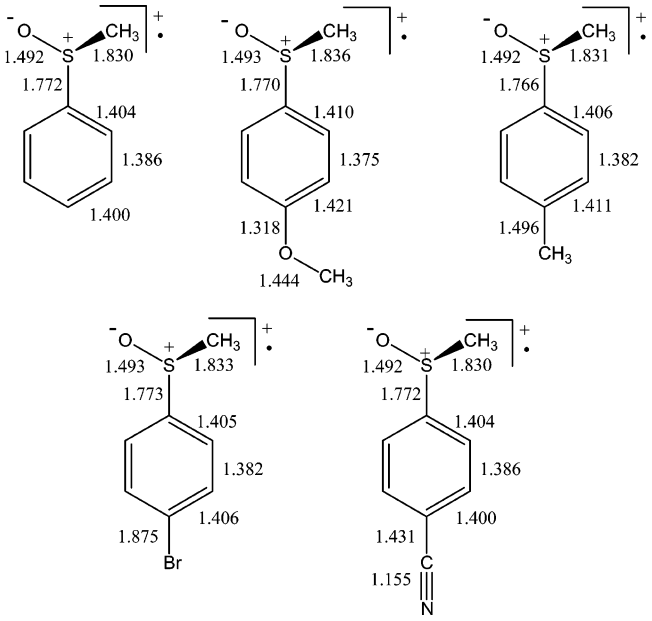

Figure 11. Bond lengths for the stable $ArSOMe^{\bullet+}$ conformers.

on sulfur and oxygen, which is in substantial agreement with the indication that in C_6H_5SOMe the highest occupied molecular orbital (HOMO) should reside on the SOMe group, being a σ^* orbital formed by the combination of S and O lone pairs.[38]

The positive charge is mainly localized on sulfur, whereas the most significant fraction of the spin is on oxygen. Thus, structure **A** in Figure 13 should be the one mainly contributing to the resonance hybrid of **1**$^{\bullet+}$. However, a very interesting observation is that a substantial fraction of both spin and charge (more than 20%) is also delocalized on the ring, particularly at the ortho and para positions. This suggests some conjugative interaction in the radical cation between the MeSO group and the ring, which might be described by structure **B** in Figure 13.

This hypothesis is consistent with the finding that such spin delocalization strongly decreases as we pass from the stable conformation **1**$^{\bullet+}$**a** (Figure 9) to the maximum energy conformation **1**$^{\bullet+}$**b** (Figure 14). Probably, this reduced spin delocalization in **1**$^{\bullet+}$**b** is at the origin of the rotational barrier around the $C_{Ar}-S$ bond mentioned above.

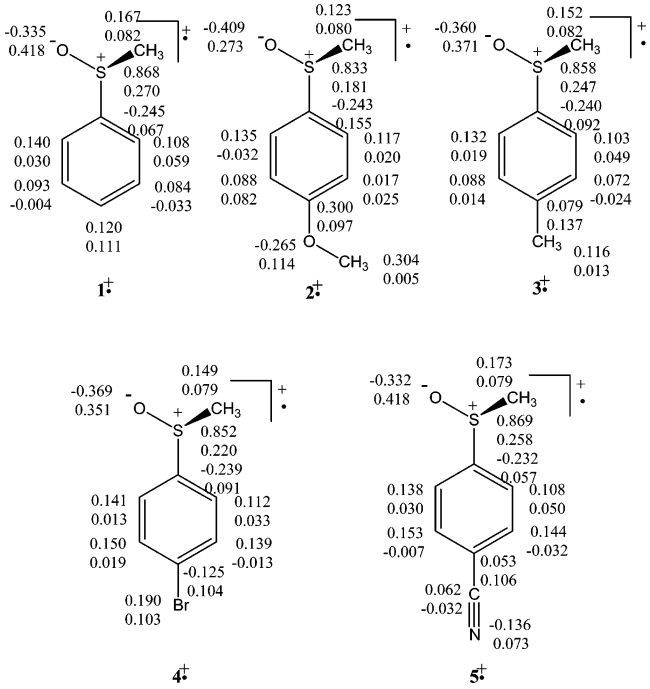

Figure 12. Mulliken charges (upper lines) and Mulliken spin populations (lower lines) for the most stable $ArSOMe^{\bullet+}$ (**1**$^{\bullet+}-$**5**$^{\bullet+}$) conformers (hydrogen atoms are summed into the attached carbon atoms).

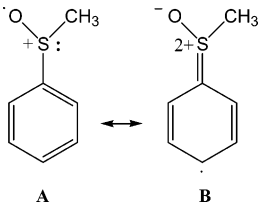

Figure 13.

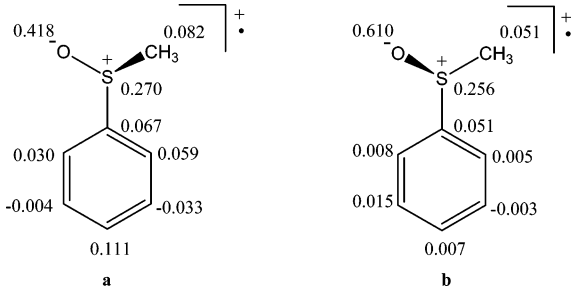

Figure 14. Spin distribution for $C_6H_5SOMe^{\bullet+}$ conformers at the minimum (a) and at the maximum of energy (b) (hydrogen atoms are summed into the attached carbon atoms).

Further support comes from the observation that the Ph−S bond distance in the stable conformation of **1**$^{\bullet+}$ (1.77 Å) is slightly shorter than that (1.83 Å) in the parent sulfoxide and that the ring in **1**$^{\bullet+}$ exhibits a slight, yet well-defined quinoid structure.

Such a conjugation appears to be significantly enhanced by the presence of the *p*-MeO group. Accordingly, **2**$^{\bullet+}$ in the stable conformation exhibits a well-defined quinoidic structure (Figure 11) and presents a large (almost 50%) extent of spin and charge delocalization in the ring (Figure 12), much higher than that of the other radical cations, which might also explain the fact that **2**$^{\bullet+}$ presents the highest rotational barrier (see Figure S21 in the Supporting Information). Even though the above picture is reasonable, it remains the puzzling finding that there are no significant changes in the S−O and Ph−S bond lengths as we

TABLE 3: Calculated Ionization Energy for 4-X−C_6H_4SOMe (1−5)

sulfoxide	IE calc (eV)
2 (X = OMe)	7.75
3 (X = Me)	8.02
1 (X = H)	8.20
4 (X = Br)	8.23
5 (X = CN)	8.59

move from $\mathbf{1}^{\bullet+}$ to $\mathbf{2}^{\bullet+}$. As in neutral sulfoxides also in the corresponding radical cations the bond distance might not be very sensitive probes for the operation of resonance effects.

In contrast with the strong electron donating para-OMe, the strong electron withdrawing para-CN in $\mathbf{5}^{\bullet+}$ does not substantially modify the charge and spin distribution observed for the unsubstituted sulfoxide radical cation in both the conformers at the minimum and at the maximum of energy (Figures 12, 14, and Figure S21 in the Supporting Information). Thus, the rotational barrier is similar for $\mathbf{1}^{\bullet+}$ and $\mathbf{5}^{\bullet+}$.

Ionization Potentials. The above discussion has shown that the greater portion of charge and spin in $ArSOMe^{\bullet+}$ is located on the SOMe group. Thus, the aryl methyl sulfoxide radical cations should be substantially seen as sulfoxide radical cations, even though with some significant charge and spin delocalization in the ring, particularly when a strong electron donating group is present.

This view is fully confirmed by the observation that the experimental ionization potential of PhSOMe (8.82 eV)[38] is lower than that of benzene (9.23 eV),[39] which clearly suggests that the electron is removed from an orbital mainly located on the SOMe group as previously concluded. On the other hand, if the electron would have been removed from the aromatic ring, then a much higher value than 9.23 eV would have been expected, given the high electron attracting power of the SOMe group (σ_p(SOMe) = 0.49).[40] For example, an IE of 9.70 has been measured for $C_6H_5CF_3$[41] ($\sigma_p(CF_3) = 0.54$[40]). Very likely, this conclusion also holds for **3**−**5**, whereas for the 4-methoxy derivative (**2**) a significant contribution of the aromatic system is probable. Accordingly, the oxidation potential of 4-$MeOC_6H_4$-SOMe (1.90 V vs SCE, see Table 1) is not much lower than that of anisole (1.96 V vs SCE).[18] On the other hand, DFT calculations have shown that in $\mathbf{2}^{\bullet+}$ there is almost 50% spin delocalization in the ring.

Finally, we have also calculated the gas-phase adiabatic ionization energy (IE), that is the difference between the total energy of the optimized neutral substrate and that of optimized radical cation (with the correction of the ZPE), for the sulfoxides investigated, and the results are listed in Table 3. The reliability of the calculated values[42] (at least for an internal comparison) is shown by the good correlation between the calculated IEs and the experimental E_p values (Table 1) ($r^2 = 0.96$) (Figure S22 in the Supporting Information).

The calculated IEs are significantly influenced by the substituent effect. Namely, the IE increases of 0.84 eV as we move from electron donating to electron withdrawing substituents, i.e., in the order MeO < Me < H < Br < CN. This increase parallels the corresponding increase in the peak oxidation potentials. The spread is larger with the ionization energies than with the oxidation potentials (0.26 eV for the same structural variation), which is probably due to the operation of a leveling effect of the solvent in the second case.

Two factors may be called into play to rationalize the substituent effects upon the ionization energies. First, the radical cation might be stabilized more by electron donating than by electron withdrawing substituents. Second, as mentioned before, going from ED to EW substituents the positive charge density on the SOMe group of the neutral sulfoxide increases which should make more difficult the removal of the electron from this group.

Summary and Conclusions

For the first time, information on spectral properties and the structure of aryl methyl sulfoxide radical cations is reported. In water, the radical cations of 4-X−C_6H_4SOMe (X = H, OMe, Me, Br, CN), generated by pulse radiolysis at pH 4, present an intense absorption in the UV region (ca 300 nm) and a broad less intense band in the visible region (between 500 and 1000 nm) whose position depends on the nature of the ring substituent. At a very low radiation dose, the radical cations decayed by first-order kinetic at a rate which increased by increasing pH. The decay probably involves a reaction of H_2O (or ^-OH) at the positively charged sulfur.

Sulfoxide radical cations were also generated in MeCN by laser flash photolysis of the neutral sulfoxides, sensitized by *N*-methylquinolinium tetrafluoroborate. In these experiments, due to the sensitizer absorption, only the longer wavelength bands of the radical cations could be observed. With all radical cations the λ_{max} value for this band was practically identical to that observed in H_2O. The decays of the radical cations followed second-order kinetics and were attributed to the back electron-transfer process.

DFT calculations (B3LYP/6-311g*) showed that, by rotation around the C_{Ar}−S bond, the energy minimum is obtained for a conformation of the radical cation where sulfur has a pyramidal geometry and the S−O bond is almost coplanar with the aromatic ring. The rotational barrier is rather low, ranging from 3.9 to 6.9 kcal/mol. Calculations also indicate that positive charge and spin densities are predominantly located on the SO group (more charge on sulfur and more spin on oxygen), but there is a substantial delocalization on the ring, around 30% for X = H, Me, Br, and CN and almost 50% for X = OMe. A conjugative interaction between the SOMe group and the aromatic π-system is suggested.

Calculations of the ionization potential of the parent sulfoxides were also performed. Values were obtained confirming that the electron is removed from the SOMe group and not from the aromatic ring, even though charge and spin are partially delocalized on the ring. The ionization potentials were found to decrease as we move from electron withdrawing to electron donating X substituents. This trend can be related to the stability of the formed radical cation or/and to the fact that as the substituent becomes more electron withdrawing the positive charge density on the SOMe group increases.

Experimental Section

Materials. Milli-Q-filtered water was used for all solutions. CH_3CN (spectrophotometric grade) and toluene were used as received. Potassium peroxydisulfate and 2-methyl-2-propanol were of the highest commercial quality available. *N*-methylquinolinium tetrafluoborate was prepared according to a literature procedure.[43] Methyl phenyl sulfoxide (**1**) and methyl *p*-tolyl sulfoxide (**3**), *p*-methoxyphenyl methyl sulfide, *p*-bromophenyl methyl sulfide, and *p*-cyanophenyl methyl sulfide are commercially available. *tert*-Butyl phenyl sulfide was prepared by the acid catalyzed reaction of thiophenol with *tert*-butyl alcohol.[44] *p*-Methoxyphenyl methyl sulfoxide (**2**), *p*-bromophenyl methyl sulfoxide (**4**), *p*-cyanophenyl methyl sulfoxide (**5**), and t*ert*-butyl phenyl sulfoxide (**6**) were prepared by reaction of the corresponding sulfides with sodium metaperiodate in

aqueous ethanol solution.[45] Phenyl trideuteriomethyl sulfoxide was synthesized according to a literature procedure.[46]

Pulse Radiolysis Experiments. The pulse radiolysis experiments were performed using a 10 MeV electron linear accelerator which supplied 0.2−2 μs pulses with doses between 2 and 20 Gy. Dosimetry was performed with N_2O-saturated 10^{-2} M aqueous KSCN solutions, for which $G[(SCN_2)^{\bullet-}] = 6.0 \times 10^{-7}$ mol J^{-1} and $\epsilon[(SCN_2)^{\bullet-}] = 7600$ M^{-1} cm^{-1} at 480 nm.[47] Experiments were performed at room temperature using argon-saturated aqueous solutions containing the substrate (0.5 mM), peroxydisulfate (5 mM), and 2-methyl-2-propanol (0.5 M). The pH of the solutions (4.0) was adjusted with $HClO_4$. A flow system was employed in all the experiments.

Laser Flash Photolysis. The excitation wavelength of 355 nm from a Nd:YAG laser (continuum, third harmonic) was used in nanosecond flash photolysis experiments (pulse width ca. 7 ns and energy < 3 mJ per pulse). The transient spectra were obtained by a point-to-point technique, monitoring the absorbance changes (ΔA) after the flash at intervals of 5−10 nm over the spectral range 350−900 nm. A 2 mL solution containing the substrate ($1.0-1.5 \times 10^{-2}$ M), NMQ^+ (3.9×10^{-4} M), and the cosensitizer (1 M toluene) was flashed in a quartz photolysis cell while nitrogen or oxygen was bubbling through them. All measurements were carried out at 22 ± 2 °C. The experimental error was ±10%.

Steady-State Photolysis. A 5 mL solution of NMQ^+ (8.6×10^{-3} M) and **3** (1.6×10^{-2} M) in N_2-saturated CH_3CN was placed in a rubber cap-sealed jacketed tube, thermostated at 25 °C, and irradiated for 10 min in a photoreactor equipped with 4 lamps (360 nm; 14 W each). An internal standard (bibenzyl) was added, and the mixture was analyzed by ^1H NMR and GC-MS. No formation of photoproducts was observed, and 98% of the unreacted substrate was recovered after the irradiation.

DFT Calculations. All computations were performed with the Gaussian 98 program[24] using the three-parameter hybrid functional B3LYP[25] with the 6-311G* basis set.[26] Such functional was chosen because it is reported to yield accurate geometries and reasonable energies.[48] Spin contamination due to states of multiplicity higher than the doublet state was negligible; the value of the $\langle S^2 \rangle$ operator was, in all cases, well within 5% of the expectation value for a doublet (0.75). Atomic charges and unpaired electron spin densities were calculated using the Mulliken population analysis. To calculate the UV absorption spectra of the investigated sulfoxide radical cations we used the time-dependent DFT method[49] (TD-DFT-B3LYP/6-311G*).

Acknowledgment. Thanks are due to the Ministero dell'Istruzione, dell'Università e della Ricerca (MIUR) and the Consiglio Nazionale delle Ricerche (CNR) for financial support. Pulse radiolysis experiments were performed at the Free Radical Research Facility of Daresbury, Cheshire, U.K. with the support of the European Commission through the Access to Large-Scale Facilities activity of the TMR Program. We thank Prof. Suppiah Navaratnam and Dr. Ruth Edge for assistance in the use of the pulse radiolysis experiments and Dr. Patrizia Gentili and Dr. Loïc Mottier for technical assistance with the cyclic voltammetry.

Supporting Information Available: Instrumentation, cyclic voltammetry, UV−vis absorption spectra of $\mathbf{1}^{\bullet+}$, $\mathbf{2}^{\bullet+}$, $\mathbf{4}^{\bullet+}$, and $\mathbf{5}^{\bullet+}$ (pulse radiolysis in H_2O), effect of pH variation on the decay of $\mathbf{1}^{\bullet+}$, laser flash photolysis of the NMQ^+/toluene/**1**−**5** systems in N_2- and O_2-saturated CH_3CN, decay of the visible absorption of $\mathbf{1}^{\bullet+}$, $\mathbf{2}^{\bullet+}$, $\mathbf{4}^{\bullet+}$, and $\mathbf{5}^{\bullet+}$ (laser flash photolysis in N_2-saturated CH_3CN), bond lengths for $\mathbf{1}^{\bullet+}$ conformers at the minimum and at the maximum of energy, spin populations for $\mathbf{2}^{\bullet+}$ and $\mathbf{5}^{\bullet+}$ conformers at the minimum and at the maximum of energy, correlation between the calculated gas-phase adiabatic ionization energy (IEs) and experimental E_p for **1**−**5**, Cartesian coordinates, and energy of neutral sulfoxides and sulfoxide radical cations. This material is available free of charge via the Internet at http://pubs.acs.org.

References and Notes

(1) Carreno, M. C. *Chem. Rev.* **1995**, *95*, 1717−1760. Fernandez, I.; Khiar, N. *Chem. Rev.* **2003**, *103*, 3651−3705.

(2) Clarke, M. J.; Zhu, F.; Frasca, D. R. *Chem. Rev.* **1999**, *99*, 2511. Lipponer, K. G.; Vogel, E.; Keppler, B. K. *Metal Based Drug* **1996**, *3*, 243. Caligaris, M.; Carugo, O. *Coord. Chem. Rev.* **1996**, *153*, 83. Shin, J. M.; Cho, Y. M.; Sachs, G. *J. Am. Chem. Soc.* **2004**, *126*, 7800−7811. Legros, J.; Dehli, J. R.; Bolm, C. *Adv. Synth. Catal.* **2005**, *347*, 19−31. Bentley, R. *Chem. Soc. Rev.* **2005**, *34*, 309−324.

(3) Mislow, K.; Schneider, P.; Ternay, A. L. *J. Am. Chem. Soc.* **1964**, *86*, 2957. Mislow, K.; Axelrod, M.; Rayner, D. R.; Gotthardt, H.; Coyne, L. M.; Hammond, G. S. *J. Am. Chem. Soc.* **1965**, *87*, 4958−4960. Cooke, R. S.; Hammond, G. S. *J. Am. Chem. Soc.* **1969**, *92*, 2739−2745. *The Chemistry of Sulfones and Sulfoxides*; Patai, S., Rappoport, Z., Stirling, C. J. M., Eds.; John Wiley & Sons: Chichester, England, 1988. Guo, Y.; Jenks, W. S. *J. Org. Chem.* **1997**, *62*, 857−864. Lee, W.; Jenks, W. S. *J. Org. Chem.* **2001**, *66*, 474−480. Vos, B. W.; Jenks, W. S. *J. Am. Chem. Soc.* **2002**, *124*, 2544−2547.

(4) Charlesworth, P.; Lee, W.; Jenks, W. S. *J. Phys. Chem.* **1996**, *100*, 15152−15155.

(5) Carlsen, L.; Egsgaard, H. *J. Am. Chem. Soc.* **1988**, *110*, 6701−6705. Kishore, K.; Asmus, K.-D. *J. Phys. Chem.* **1991**, *95*, 7233−7239, and references therein.

(6) Only the studies by Rajagopal et al.[8] have so far dealt with aromatic sulfoxide radical cations, but the detection and spectral characterization of the aromatic sulfoxide radical cation intermediate are rather uncertain.

(7) Adaikalasamy, K.; Venkataramanan, N. S.; Rajagopal, S. *Tetrahedron* **2003**, *59*, 3613−3619.

(8) Ganesan, M.; Sivasubramanian, V. K.; Rajagopal, S.; Ramaraj, R. *Tetrahedron* **2004**, *60*, 1921−1929.

(9) Watanabe, Y.; Iyanagi, T.; Oae, S. *Tetrahedron Lett.* **1982**, *23*, 533−536.

(10) Baciocchi, E. *Acta Chem. Scand.* **1990**, *44*, 645−652. Baciocchi, E.; Del Giacco, T.; Elisei, F. *J. Am. Chem. Soc.* **1993**, *115*, 12290−12295. Baciocchi, E.; Lanzalunga, O.; Malandrucco, S.; Ioele, M.; Steenken, S. *J. Am. Chem. Soc.* **1996**, *118*, 8973−8974. Ioele, M.; Steenken, S.; Baciocchi, E. *J. Phys. Chem. A* **1997**, *101*, 2979−2987. Baciocchi, E.; Bietti, M.; Lanzalunga, O.; Steenken, S. *J. Am. Chem. Soc.* **1998**, *120*, 11516−11517. Baciocchi, E.; Bietti, M.; Manduchi, L.; Steenken, S. *J. Am. Chem. Soc.* **1999**, *121*, 6624−6629. Baciocchi, E.; Bietti, M.; Lanzalunga, O. *Acc. Chem. Res.* **2000**, *33*, 243−251. Baciocchi, E.; Del Giacco, T.; Elisei, F.; Gerini, M. F.; Lapi, A.; Liberali, P.; Uzzoli, B. *J. Org. Chem.* **2004**, *69*, 8323−8330. Baciocchi, E.; Gerini, M. F. *J. Phys. Chem. A* **2004**, *108*, 2332−2338. Baciocchi, E.; Del Giacco, T.; Elisei, F.; Lapi, A. *J. Org. Chem.* **2006**, *71*, 853−860. Baciocchi, E.; Del Giacco, T.; Gerini, M. F.; Lanzalunga, O. *Org. Lett.* **2006**, *8*, 641−644.

(11) Kishore, K.; Asmus, K.-D. *J. Chem. Soc., Perkin Trans. 2* **1989**, 2079−2084.

(12) Eberson, L. *Adv. Phys. Org. Chem.* **1982**, *18*, 79.

(13) Buxton, G. V.; Greenstock, C. L.; Helman, W. P.; Ross, A. B. *J. Phys. Chem. Ref. Data* **1988**, *17*, 513−886.

(14) Molar extinction coefficients of radical cations $\mathbf{1}^{\bullet+}$−$\mathbf{5}^{\bullet+}$ have not been determined since, as observed in aliphatic sulfoxide radical cation,[11] the yield of aromatic sulfoxide radical cations might be lower than the maximum possible yields which corresponds to that of $SO_4^{\bullet-}$ ($G = 2.7$).

(15) Preliminary time-dependent DFT calculations carried out at the DFT geometry corresponding to the minimum energy of the aromatic sulfoxide radical cations (vide infra) have confirmed that these species should exhibit an UV−visible spectrum with two bands, one around 300 nm, the other at a longer wavelength (550−900 nm). Calculations also indicated that the absorptions observed in the region 500−1000 nm are essentially related to the electronic transitions from the occupied MOs (SOMO-1 or lower orbitals), mainly delocalized on the aromatic moiety, to the delocalized unoccupied orbital (LUMO), involving the SOMe group to a considerable extent. The theoretical calculations roughly reproduced the experimental UV spectra obtained in aqueous solution by pulse radiolysis. For example the λ_{max} of the UV and visible absorption bands calculated for $\mathbf{3}^{\bullet+}$ are 318 and 821 nm, respectively. The theoretical study of the spectral properties of aromatic sulfoxide radical cations is in progress, and the results will be reported in a separate publication.

(16) Dockery, K. P.; Dinnocenzo, J. P.; Farid, S.; Goodman, J. L.; Gould, I. R.; Todd, W. P. *J. Am. Chem. Soc.* **1997**, *119*, 1876−1883.

(17) The only exception was 4-$CNC_6H_4SOCH_3^{\bullet+}$ as its reduction potential is not significantly lower than that of toluene (E_p 2.39 V vs SCE in MeCN).[18]

(18) Fukuzumi, S.; Kochi, J. K. *J. Am. Chem. Soc.* **1981**, *103*, 7240−7252.

(19) Bockman, T. M.; Kochi, J. K. *J. Am. Chem. Soc.* **1989**, *111*, 4669−4683.

(20) O'Neill, P.; Steenken, S.; Schulte-Frohlinde, D. *J. Phys. Chem.* **1975**, *79*, 2773−2779.

(21) Shukla, D.; Liu, G.; Dinnocenzo, J. P.; Farid, S. *Can. J. Chem.* **2003**, *81*, 744−757.

(22) The extinction coefficient of $NMQ^{\bullet}$ at $\lambda_{max} = 540$ nm was obtained from the absorption spectrum of the NMQ radical and biphenyl (BP) radical cation recorded after laser irradiation of the NMQ^+/BP system in CH_3CN. Taking into account that the two transients have the same concentration and the absorption coefficient of $BP^{\bullet+}$ at $\lambda_{max} = 670$ nm is 14 500 M^{-1} cm^{-1},[23] ϵ is calculated by the equation: $\epsilon_{540}(NMQ^{\bullet}) = \epsilon_{670}(BP^{\bullet+}) \times \Delta A_{540}(NMQ^{\bullet})/\Delta A_{670}(BP^{\bullet+})$.

(23) Gould, I. R.; Ege, D.; Moser, J. E.; Farid, S. *J. Am. Chem. Soc.* **1990**, *112*, 4290−4301.

(24) Frisch, M. J.; Trucks, G. W.; Schlegel, H. B.; Scuseria, G. E.; Robb, M. A.; Cheeseman, J. R.; Zakrzewski, V. G.; Montgomery, J. A., Jr.; Stratmann, R. E.; Burant, J. C.; Dapprich, S.; Millam, J. M.; Daniels, A. D.; Kudin, K. N.; Strain, M. C.; Farkas, O.; Tomasi, J.; Barone, V.; Cossi, M.; Cammi, R.; Mennucci, B.; Pomelli, C.; Adamo, C.; Clifford, S.; Ochterski, J.; Petersson, G. A.; Ayala, P. Y.; Cui, Q.; Morokuma, K.; Malick, D. K.; Rabuck, A. D.; Raghavachari, K.; Foresman, J. B.; Cioslowski, J.; Ortiz, J. V.; Stefanov, B. B.; Liu, G.; Liashenko, A.; Piskorz, P.; Komaromi, I.; Gomperts, R.; Martin, R. L.; Fox, D. J.; Keith, T.; Al-Laham, M. A.; Peng, C. Y.; Nanayakkara, A.; Gonzalez, C.; Challacombe, M.; Gill, P. M. W.; Johnson, B.; Chen, W.; Wong, M. W.; Andres, J. L.; Gonzalez, C.; Head-Gordon, M.; Replogle, E. S.; Pople, J. A. *Gaussian 98*, *revision A.7*; Gaussian, Inc.: Pittsburgh, PA, 1998.

(25) Lee, C.; Yang, W.; Parr, R. G. *Phys. Rev. B: Condens. Matter* **1988**, *37*, 785−789. Becke, A. D. *J. Chem. Phys.* **1993**, *98*, 5648−5652.

(26) Hehre, W. J.; Radom, L.; Schleyer, P. v. R.; Pople, J. A. *Ab Initio Molecular Orbital Theory*; J. Wiley & Sons: New York, 1987.

(27) Bally, T.; Borden, W. T. *Rev. Comput. Chem.* **1999**, *13*, 1−97.

(28) Buchanan, G. W.; Reyes-Zamora, C.; Clarke, D. E. *Can. J. Chem.* **1974**, *52*, 3895.

(29) Bzhezovskii, V. M.; Il'chenko, N. N.; Chura, M. B.; Gorb, L. G.; Yagupol'skii, L. M. *Russ. J. Gen. Chem.* **2005**, *75*, 86−93.

(30) Benassi, R.; Mucci, A.; Schenetti, L.; Taddei , F. *J. Mol. Struct. (THEOCHEM)* **1989**, *184*, 261−268.

(31) Butenko, G. G.; Vereshchagin, A. N.; Abunagimova, R. Kh. *Izv. Akad. Nauk. SSSR* **1981**, 2054.

(32) The calculated geometrical features of neutral C_6H_5SOMe in the minimum energy conformation are similar to those calculated by Bzhezovskii et al.[29] at the MP2/6-31+G* level.

(33) The S−O bond distance in dimethyl sulfoxide was calculated with the same method (B3LYP/6-311G*) applied for calculations on C_6H_5SOMe (see the Supporting Information).

(34) However, the S−O bond length in a series of sulfoxides included in a formally aromatic ring has been found to be little influenced by the degree of aromaticity of the system.[35]

(35) Jenks, W. S.; Matsunaga, N.; Gordon, M. *J. Org. Chem.* **1996**, *61*, 1275−1283.

(36) Rosini, C.; Donnoli, M. I.; Superchi, S. *Chem. Eur. J.* **2001**, *7*, 72−78.

(37) Herron, J. T. In *The Chemistry of Sulfones and Sulfoxides*; Patai, S., Rappoport, Z., Stirling, C. J. M., Eds.; John Wiley & Sons: Chichester, England, 1988; Chapter 4.

(38) Csonka, I. P.; Vass, G.; Szepes, L.; Szabó, D.; Kapovits, I. *J. Mol. Struct. (THEOCHEM)* **1998**, *455*, 141−159.

(39) Fukuzumi, S.; Kochi, J. K. *J. Org. Chem.* **1981**, *46*, 4116−4126.

(40) McDaniel, D. H.; Brown, H. C. *J. Org. Chem.* **1958**, *23*, 420.

(41) Turner, D. W.; Baker, C.; Baker, A. D.; Brundle, C. R. *Molecular Photoelectron Spectroscopy*; Wiley-Interscience: London, 1970.

(42) IEs can be computed by DFT methods to a reasonable accuracy, see: Curtiss, L. A.; Redferm, P. C.; Raghavachari, K.; Pople, J. A. *J. Am. Chem. Soc.* **1987**, *109*, 9, 42. Lin, J. L.; Huang, L. C. L.; Tzeng, W. B. *J. Phys. Chem. A* **2001**, *105*, 11455−11461.

(43) Donovan, P. F.; Conley, D. A. *J. Chem. Eng. Data* **1966**, *11*, 614−615.

(44) Cutress, N. C.; Grindley, T. B.; Katritzky, A. R.; Topsom, R. D. *J. Chem. Soc., Perkin Trans. 2* **1974**, 263−268.

(45) Johnson, C. R.; Leonard, N. J. *J. Org. Chem.* **1962**, *27*, 282−284.

(46) González-Núñez, M. E.; Mello, R.; Royo, J.; Ríos, J. V.; Asensio, G. *J. Am. Chem. Soc.* **2002**, *124*, 9154−9163.

(47) Schuler, R. H.; Hartzell, A. L.; Behar, B. *J. Phys. Chem.* **1981**, *85*, 192.

(48) Curtiss, L. A.; Raghavachari, K.; Redfern, P. C.; Pople, J. A. *J. Chem. Phys.* **1997**, *106*, 1063−1079. Arulmozhiraja, S.; Sato, T.; Yabe, A. *J. Comput. Chem.* **2001**, *22*, 923−930. Kraka, E.; Cremer, D. *J. Comput. Chem.* **2001**, *22*, 216−220. Johnson, W. T. G.; Cramer, C. J. *J. Am. Chem. Soc.* **2001**, *123*, 923−928.

(49) (a) Gross, E. K. U.; Kohn, W. *Adv. Quantum Chem.* **1990**, *21*, 255. (b) Casida, M. E. In *Recent Advances in Density Functional Methods*; Chong, D. P., Ed.; World Scientific: Singapore, 1995, Vol. 1. (c) Wiberg, K. B.; Stratmann, R. E.; Frisch, M. J. *Chem. Phys. Lett.* **1998**, *297*, 60.